NANO · MICRO small
www.small-journal.com

Polymerization Based on Modified β-Cyclodextrin Achieves Efficient Phosphorescence Energy Transfer for Anti-Counterfeiting

Qingwen Cheng, Xin-Kun Ma, Xiaolu Zhou, Ying-Ming Zhang, and Yu Liu**

Supramolecular polymerization can not only activate guest phosphorescence, but also promote phosphorescence Förster resonance energy transfer and induce effective delayed fluorescence. Herein, the solid supramolecular assemblies of ternary copolymers based on acrylamide, modified β-cyclodextrin (CD), and carbazole (CZ) are reported. After doping with polyvinyl alcohol (PVA) and dyes, a NIR luminescence supramolecular composite with a lifetime of 1.07 s, an energy transfer efficiency of up to 97.4% is achieved through tandem phosphorescence energy transfer. The ternary copolymers can realize macrocyclic enrichment of dyes in comparison to CZ and acrylamide copolymers without CD, which can facilitate energy transfer between triplet and singlet with a high donor–acceptor ratio. Additionally, the flexible polymeric films exhibit regulable lifetime, tunable luminescence color, and repeatable switchable afterglow by adjusting the excitation wavelength, donor–acceptor ratio, and wet/dry stimuli. The luminescence materials are successfully applied to information encryption and anti-counterfeiting.

1. Introduction

The development of ultralong lifetime luminescence, especially organic room-temperature phosphorescence, can provide a new perspective for encryption and anti-counterfeiting.[1–5] Many excellent methods have been developed to enhance the phosphorescence properties, such as crystallization, polymerization, and supramolecular assembly.[6–8] Specifically, macrocyclic restricted supramolecular assembly has become a preferred option for creating high-efficiency phosphorescent materials. And it has been shown that incorporating multiple interactions is an effective strategy for attaining extremely efficient phosphorescent performance.

Förster resonance energy transfer (FRET) is regarded as a preference for obtaining multicolored materials by matching the energy of the donor and acceptor.[9–13] Phosphorescence resonance energy transfer (PRET) is a process in which the phosphorescent energy transfer from the donor to the acceptor can be achieved when the donor's phosphorescent spectrum overlaps with the acceptor's absorption spectrum and the distance is ≈1–10 nm, which facilitates red-shifted emission and long-lived luminescence when compared to fluorescence energy transfer.[14–20] George et al. reported a highly effective room temperature phosphorescence in solution, in which hydrogels were formed by immobilizing phthalimide phosphor on supramolecular compounds; it serves as a platform for light-harvesting to produce delayed fluorescence.[21] It is an art of balancing to design a high-efficiency donor–acceptor (D–A) energy transfer system, because high receptor concentrations are necessary to ensure the minimum distance between D–A, particularly in multi-step energy transfer systems.[22–27] In contrast, phosphorescence energy transfer systems are prone to quenching induced by aggregation of phosphors.[28–33] Macrocycles such as cyclodextrins and cucurbiturils could specifically bond guest molecules into cavity, which provides a possibility to enrich D–A chromophores at low concentrations and effectively prevents aggregation quenching.[34–37] Therefore, we assume whether the energy transfer efficiency can be improved by reducing the distance between the donor and acceptor through supramolecular assembling, thus achieving more efficient multi-step energy transfer with less lifetime loss at low-concentration doping scenarios.

To validate our hypothesis, we designed and synthesized polyacrylamide (P_1) composed of modified β-cyclodextrin (CD) and carbazole (CZ), and the self-assembled polymeric spherical nanoparticles were doped into polyvinyl alcohol (PVA), P_1/PVA displayed impressive ultralong blue phosphorescence with 2.92 s lifetime. Notably, P_1 as the energy donor, with a high donor/acceptor ratio after assembling with rhodamine B (RhB), effective phosphorescence resonance energy transfer (PRET) can be accomplished (RhB, [D]:[A] ≥ 100:20, **Scheme 1**). Compared with free-doping, P_1/PVA required fewer receptors to achieve afterglow color conversion and suffered less lifetime loss. The supramolecular enrichment is more pronounced in the second energy transfer. Concretely, with further assembling with NIR dye Cy5, the polymeric films displayed ultralong lifetime NIR

Q. Cheng, X.-K. Ma, X. Zhou, Y.-M. Zhang, Y. Liu
College of Chemistry State Key Laboratory of Elemento-Organic Chemistry
Nankai University
Tianjin 300071, P. R. China
E-mail: ymzhang@nankai.edu.cn; yuliu@nankai.edu.cn

The ORCID identification number(s) for the author(s) of this article can be found under https://doi.org/10.1002/smll.202309732

DOI: 10.1002/smll.202309732

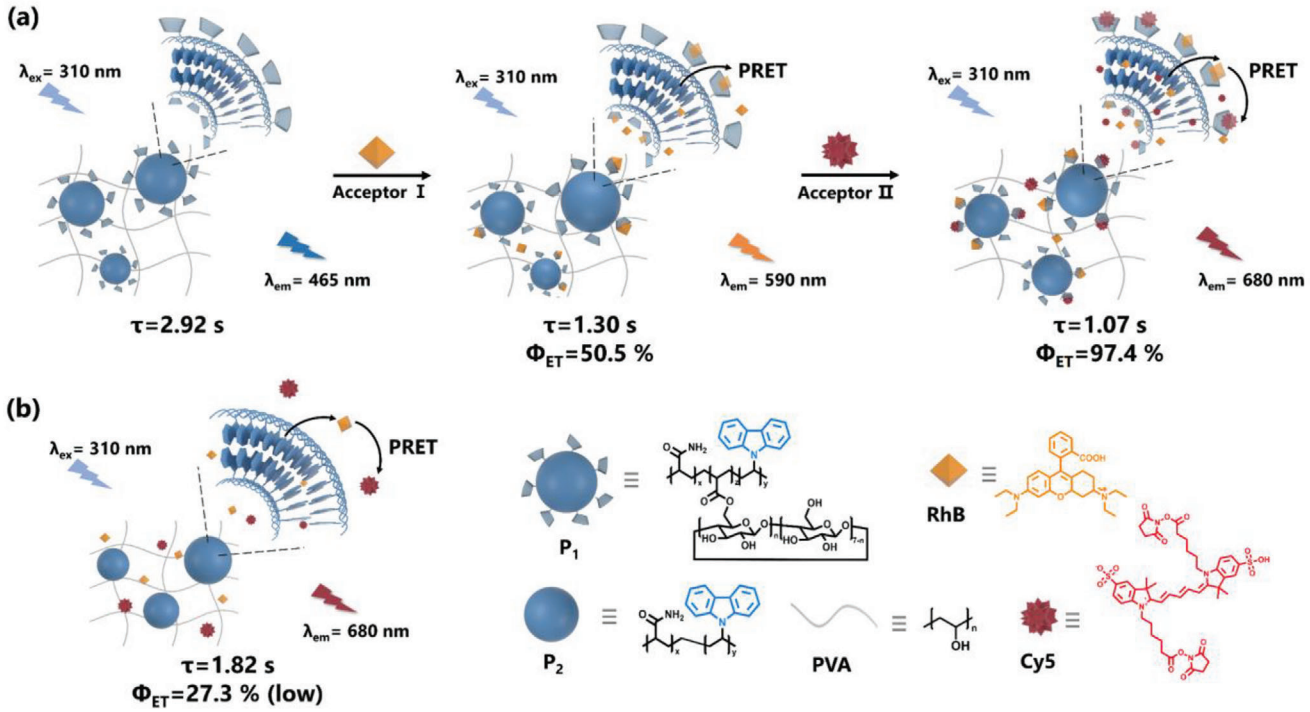

Scheme 1. Schematic illustration of a) the multilevel assembly mechanism of P_1, RhB, and Cy5; b) a multi-component supramolecular system without CD.

afterglow with a lifetime of 1.07 s and energy transfer efficiency of up to 97.4%, which is the highest recorded result for the reported phosphorescence cascade energy transfer system (Figure S1 and Table S1, Supporting Information). Remarkably, the luminescence color and lifetime could be facilely regulated by adjusting the excitation wavelength, D–A ratio, and wet/dry stimuli could repeatedly switch the luminous. Owing to tunable multidimensional luminescence, these polymeric materials can be fabricated into different shapes of films and security inks with multifunctional applications. A fresh perspective on the creation of sophisticated multicolor afterglow materials is offered by the macrocycle-confined solid supramolecular strategy.

2. Results and Discussion

CD were synthesized and confirmed structure by ^{1}H NMR and IR (Figure S2, Supporting Information),[38,39] and P_1 was proved by ^{1}H NMR and gel permeation chromatography (GPC) (**Figure 1**a; Figures S3 and S4 and Table S2, Supporting Information). The work was based on a fixed mass ratio of P_1 and PVA, which is 10:1. All films are thoroughly dried before testing. P_2/PVA films exhibited phosphorescence peaks ≈416, 442, and 465 nm (Figure 1b). The different ratio of CZ was first compared; the intensity of the characteristic peak reached the highest when the ratio of CZ was 5% (Figure S5, Supporting Information). Next, P_1/PVA films showed little influence on the luminescence properties of the donor with the addition of CD, and the lifetime at 465 nm increased from 2.28 to 2.92 s (Figure 1c; Figure S6, Supporting Information). We fixed the P_1 as the CD is added at 15% and the CZ at 5% when performing polymerization reactions.

To achieve afterglow color conversion, dye RhB was chosen as acceptor. Since the premise of energy transfer is satisfied, its absorption spectrum has a good overlap with the phosphorescence spectrum of P_1/PVA films (**Figure 2**a). The intensity of the P_1/PVA@RhB films at 590 nm increased gradually with the ratio of RhB increased, this implied a high-efficiency energy transfer, which can be found that the peak at 590 nm reached the highest when the ratio is 100:20 (Figure 2b). The lifetime at 465 nm of P_1/PVA@RhB films was reduced from 2.92 to 1.46 s after the [D]:[A] up to 100:20, and the lifetime at 590 nm of the P_1/PVA@RhB films was 1.30 s (Figures S7 and S8 and Table S3, Supporting Information). The decrease was consistent with the PRET from the donor's triplet to the acceptor's singlet. It should be noted that after the exciting light was turned off, P_1/PVA@RhB films emitted ultralong orange–red afterglow that was visible to the naked eye for 6 s (Figure 2e). As an essential criterion to evaluate the efficiency of phosphorescence-capturing system, Φ_{ET} value was determined as 50.5% when [D]:[A] = 100:20 (Figure 2c). Then, the RhB was introduced into different CD ratios of P_1/PVA films as a control experiment when [D]:[A] is fixed at 100:20, the emission peak at 590 nm was increased nine times as the proportion of CD increases from 0% to 5% (Figure 2d). This implies the enrichment of cyclodextrin makes the D–A more compact and improves energy transfer efficiency. Similarly, fluorescein sodium (Flu) was applied as an accepter to verify the universality of this phosphorescence-capturing platform. Not surprisingly, the characteristic peak of 525 nm belonging to Flu gradually appears with the addition of

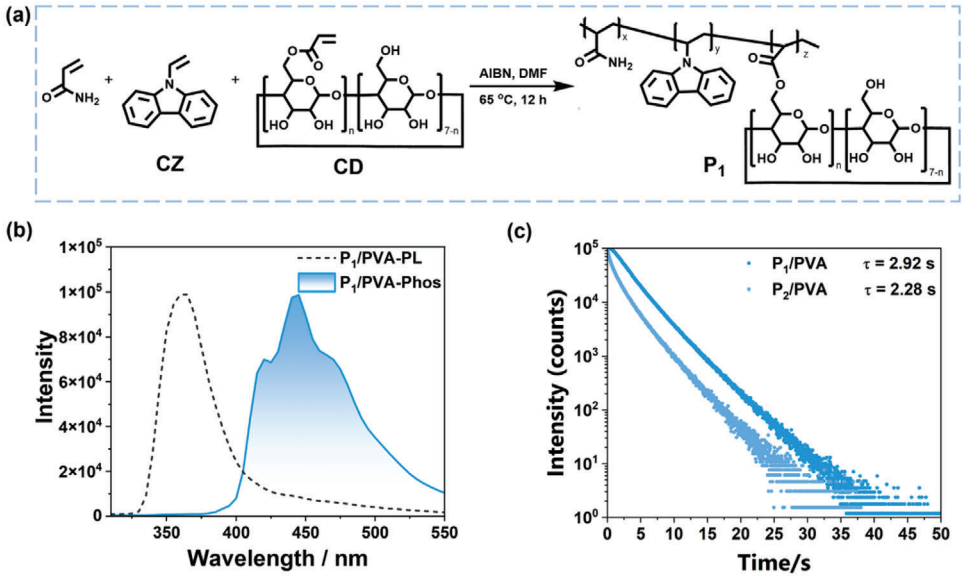

Figure 1. a) Synthetic route of P_1; b) PL spectrum and phosphorescence spectrum of P_1/PVA film; c) Time-resolved decay spectra of P_1/PVA and P_2/PVA films at 465 nm at 298 K (m_{CZ}:m_{PVA} = 10:1, λ_{ex} = 290 nm, delayed time = 100 µs).

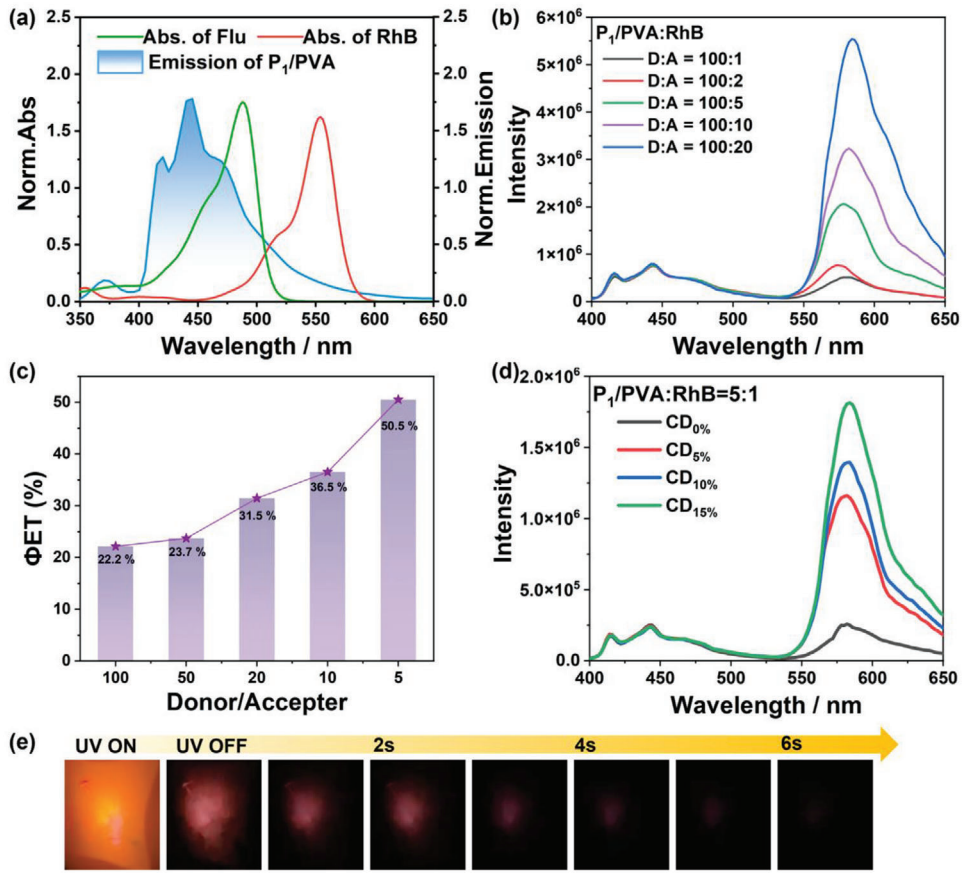

Figure 2. a) Absorption spectra of RhB, Flu and normalized emission spectrum of P_1/PVA film; b) Delayed emission spectra of P_1/PVA@RhB films at various donor/acceptor ratios; c) The Φ_{ET} values of P_1/PVA@RhB films at different donor/acceptor ratios which were calculated by the phosphorescence lifetimes data; d) Delayed emission spectra of P_1/PVA films with the increment of CD proportion; e) luminescence photographs of P_1/PVA@RhB film before and after the 300 nm UV lamp was turned off (m_{CZ}:m_{PVA} = 10:1, [P_1]:[RhB] = 100:20, λ_{ex} = 290 nm, delayed time = 100 µs).

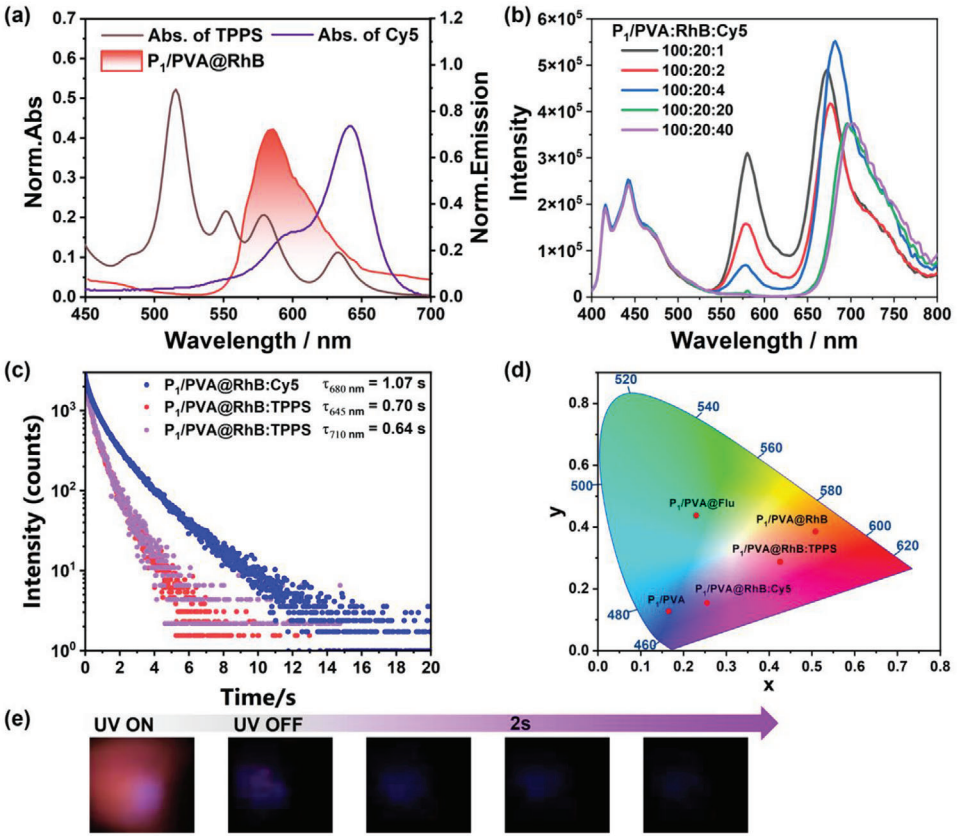

Figure 3. a) Absorption spectra of Cy5, TPPS and normalized emission spectrum of P_1/PVA@RhB film; b) Delayed emission spectra of P_1/PVA@RhB:Cy5 films at different donor/acceptor ratios; c) Time-resolved decay spectra of P_1/PVA@RhB, P_1/PVA@RhB:Cy5, P_1/PVA@RhB:TPPS films at 680, 645, and 710 nm; d) CIE 1931 chromaticity diagram of P_1/PVA, P_1/PVA@RhB, P_1/PVA@Flu, P_1/PVA@RhB:Cy5 and P_1/PVA@RhB:TPPS films at 298K; e) luminescence photographs of P_1/PVA@RhB:Cy5 film before and after turning off 300 nm UV (m_{CZ}:m_{PVA} = 10:1, [P_1/PVA]:[RhB]:[Cy5] = 100:20:4, [P_1/PVA]:[RhB]:[TPPS] = 100:20:20, λ_{ex} = 290 nm, delayed time = 100 μs).

Flu (Figure S9, Supporting Information). The lifetime at 465 nm of P_1/PVA@Flu film was measured as 1.98 s when [D]:[A] = 100:20, and the lifetime at 525 nm was 1.86 s (Figures S7 and S10, Supporting Information). The value of Φ_{ET} was determined as 35.9% according to the deceased donor's intensity data (Figure S12, Supporting Information). In addition, the energy transfer effect of P_1/PVA@RhB films was significantly higher than P_1/PVA@Flu films when the intensity of emission at 465 nm and the donor/acceptor ratio were at the same level (Figure S11, Supporting Information); this might be attributed to the better overlap between RhB absorption and the donor luminescence.

Considering the light-harvesting system consists of multiple multi-colored components in nature and is used for multi-step sequential energy transfer instead of one-step energy transfer,[40–42] we further researched the potential of cascade energy transfer processes in supramolecular aggregate P_1/PVA@RhB system. Hydrophobic dye molecules Cy5, which has long alkyl chains, and tetrasodium 5,10,15,20-tetrakis(4-sulfophenyl)porphyrin (TPPS), contains porphyrin macrocycles that can interact with guest molecules were selected. The absorption spectra and the P_1/PVA@RhB system's emission spectrum had good spectral overlaps (**Figure 3**a). The P_1/PVA@RhB system's emission at 590 nm diminished with the addition of the Cy5, and a new emission peak at 680 nm emerged, indicating that there is a PRET from the singlet of RhB to singlet of Cy5 (Figure 3b). One explanation is primary energy transfer from P_1/PVA system to RhB had high energy transfer efficiency, and P_1/PVA films phosphorescence emission at 465 nm was significantly quenched; another is the absorption spectra of P_1/PVA system have a smaller overlap with Cy5 than with RhB. In time-resolved decay spectra, P_1/PVA@RhB: Cy5 films at 590 nm decreased to 1.05 s, and the lifetime at 680 nm ascribed to Cy5 was 1.07 s (Figure 3c; Figure S18, Supporting Information). The P_1/PVA@RhB:Cy5 films emitted ultralong purple afterglow after turning off the exciting light, which could be observed lasting for 3 s by the naked eye (Figure 3e). According to the deceased donor's intensity data at 590 nm, The value of Φ_{ET} was calculated to be 97.4% when the P_1/PVA to RhB to Cy5 molar ratio of 100:20:4 (Figure S13, Supporting Information). Another NIR luminescence receptor, TPPS was introduced into the P_1/PVA@RhB system to demonstrate the versatility of energy transfer system. Upon the stepwise addition of TPPS, the double emissions of TPPS were observed at 645 and 710 nm (Figure S17, Supporting Information). The lifetime of P_1/PVA@RhB:TPPS films at 590 nm declined to 0.57 s, and the lifetimes at 645 and 710 nm belonging to TPPS were 0.70 and 0.64 s (Figure 3c; Figure S18, Supporting Information). Additionally, the value of Φ_{ET} was

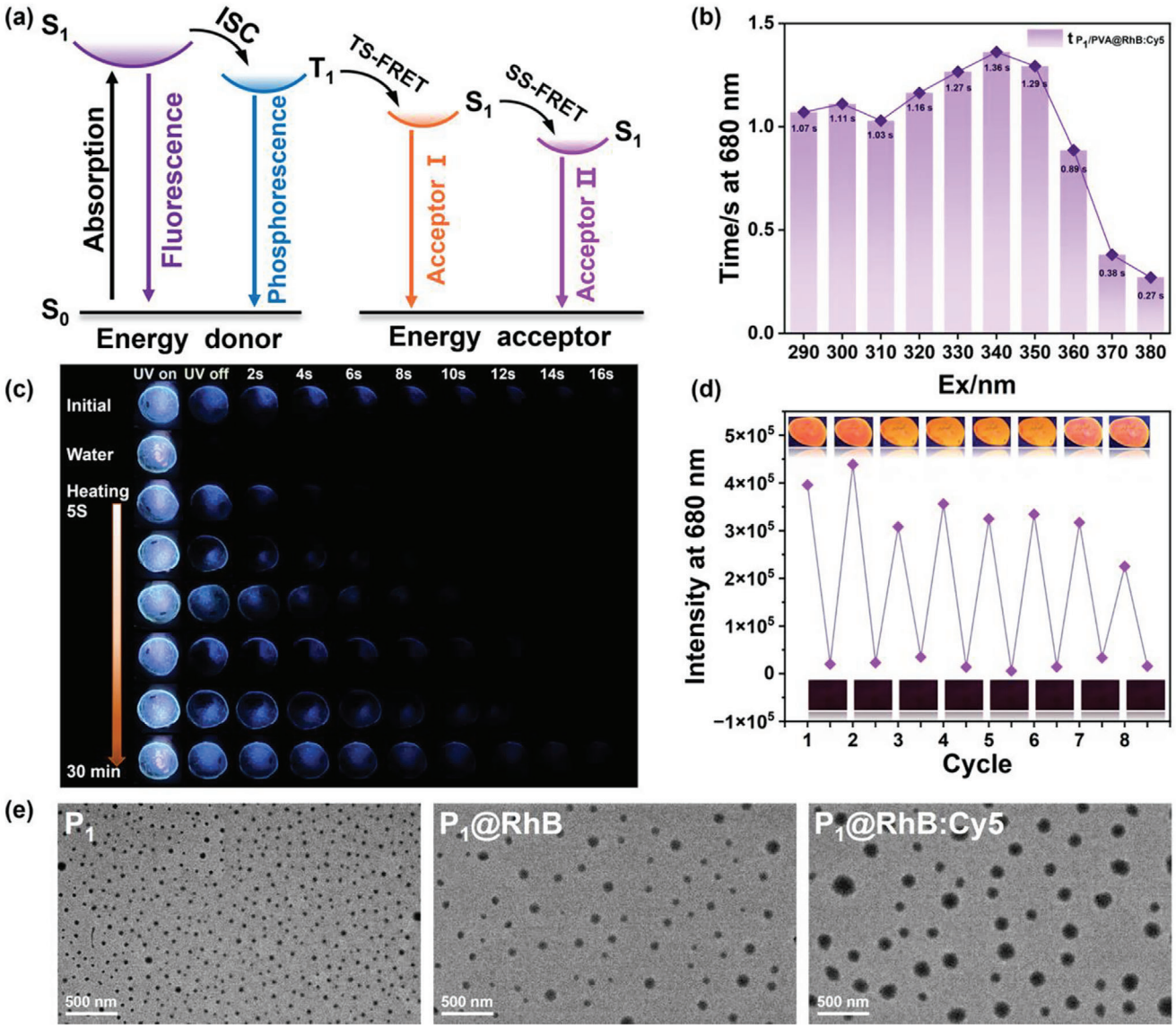

Figure 4. a) Possible mechanisms of cascade phosphorescence capture processes (ISC = intersystem crossing, TS-FRET = Triplet to singlet Förster resonance energy transfer, SS-FRET = Singlet to singlet Förster resonance energy transfer); b) The lifetimes at 680 nm of P_1/PVA@RhB:Cy5 films at different excitation wavelengths ([P_1]:[RhB]:[Cy5] = 100:20:4, λ_{ex} = 290 nm, delayed time = 100 μs); c) Photographs of water-sprayed P_1/PVA film heated for different times; d) Repeated cycles of the wet/dry processes and the corresponding photographs of P_1/PVA@RhB:Cy5 film after turning off the UV light ([P_1]:[RhB]:[Cy5] = 100:20:4, m_{CZ}:m_{PVA} = 10:1); e) TEM images of P_1 (left), P_1@RhB (middle) and P_1@RhB:Cy5 ([c] = 10^{-3} M, [P_1]:[RhB]:[Cy5] = 100:1:1, scale bar: 500 nm).

88.4% according to the change of intensity at 590 nm when the molar ratio of P_1/PVA to RhB to TPPS is 100:20:20 (Figure S14, Supporting Information). It is worth mentioning that P_1/PVA system can be used as a long-life phosphorescent donor material. With energy receptor dyes adding, P_1/PVA@RhB, P_1/PVA@Flu, P_1/PVA@RhB:Cy5, and P_1/PVA@RhB:TPPS showed luminous color transitions from blue to green or orange, and then eventually to purple (Figure 3d). Additionally, there is a potential mechanism for the cascaded phosphorescence-capturing system (**Figure 4**a), which involves a two-step energy transfer procedure called TS-FRET and SS-FRET to achieve the emission of primary and secondary receptors.

To thoroughly verify the enrichment effect of CD, the control experiments in the P_2/PVA@RhB and P_2/PVA@RhB:Cy5 systems were done ([P_2/PVA]:[RhB]:[Cy5] = 100:20:4). The characteristic lifetime of P_2/PVA@RhB and P_2/PVA@RhB:Cy5 films at 590 and 680 nm were 1.97 and 1.82 s (Figure S19, Supporting Information). The co-assembly P_2/PVA@RhB:Cy5 in the absence of CD can emit weak phosphorescence because polymer encase dyes can induce PRET in 1–10 nm. And the characteristic peaks of Cy5 were five times more substantial while the CD existed (Figure S20, Supporting Information). This is because the host-guest interactions between dyes and CD can further confine dyes, restrain the non-radiative transitions and

efficiently enhance the phosphorescence. More importantly, the doping ratio of the P_1/PVA@RhB:Cy5 system is only 100:20:2, while the P_2/PVA@RhB:Cy5 system without CD requires a ratio of 100:20:20 to achieve a similar energy transfer effect (Figure S21, Supporting Information). In addition, the Φ_{ET} of P_2/PVA@RhB and P_2/PVA@RhB:Cy5 systems are much smaller, which are only 3.95% and 27.3% separately (Figures S15 and S16, Supporting Information). In a word, the presence of macrocycles significantly improves energy transfer efficiency and reduces the doping ratio. Transmission electron microscopy (TEM) showed that with the addition of dye, the nanoparticles are gradually enlarged (Figure 4e). The PVA assemblies tend to same result (Figure S22, Supporting Information). The results of the TEM image also confirm the encapsulation effect of the macrocyclic on the dyes.

The PVA-based mixture doped with natural β-cyclodextrin and carbazole was prepared. It was found that the enrichment effect of non-covalent interaction was worse than the effect of covalent bonding on the polymer (Figure S23, Supporting Information). The sodium adamantane-1-carboxylate (AdCOONa) was introduced as the competitive guest of the CD cavity to improve the necessary host-guest interaction further. After the AdCOONa was doping into the P_1/PVA@RhB system, it was found that the characteristic absorption peak at 590 nm decreased significantly without enrichment effect (Figure S23, Supporting Information). ^{1}H NMR and 2D Noesy strongly provided evidence that CZ and CD in the polymer don't interact (Figures S24 and S25, Supporting Information). Furthermore, the host-guest binding behavior between dyes and β-CD was measured by ^{1}H NMR and UV–vis spectroscopic experiments. In Figure S26 (Supporting Information), the protons of the aromatic region of dyes underwent remarkable shifts. The binding constant (K_S) of Flu, RhB, Cy5, and TPPS with β-CD were respectively determined to be 126, 7285, 5530, and 17 430 M^{-1} through using the nonlinear least-squares fitting method (Figure S27, Supporting Information). These also explain why the P_1/PVA@RhB film's energy transfer is better than the P_1/PVA@Flu system, while the Flu's spectra overlap is better. We found that RhB was a crucial step in achieving the cascade phosphorescence-capturing because of its excellent absorption and emission properties. Cy5 was introduced to the P_1/PVA system, but there was barely any Cy5 emission at 680 nm, showing that there was no efficient energy transfer between them (Figure S28, Supporting Information). Furthermore, the emission at 465 nm maintains essentially unaltered, which implies that little energy transfer from the P_1/PVA assembly to the secondary receptor.

When the excitation wavelength is changed from 290 to 480 nm, the lifetime of P_1/PVA@RhB:Cy5 film at 680 nm rises significantly, from 1.07 s at the beginning to a maximum of 1.36 s at 340 nm and then plummets until it disappears (Figure 4b; Figure S29, Supporting Information). At the same time, the changing trend of a lifetime can be seen in the pictures under different excitation wavelengths, and their colors also change from purple to blue (Figure S30, Supporting Information). These may indicate that the characteristic peaks displayed by the receptors come from energy transfer from donor. Additionally, stimuli-responsive luminescent films have great potential for development in anti-counterfeiting areas, humidity is a powerful moderator of phosphorescence.[43–48] To validate that humidity influences our polymeric system, the emission spectrum and P_1/PVA film's corresponding lifetimes were tested at different degrees of wet/dry stimuli. First, watering film was measured and found no phosphorescence emission at 465 nm (Figure 4c). The wet/dry effect was explored using a hair dryer for heat up for different times. The intensity of the 465 nm emission band gradually recovers with the heating time. When the heating time was 30 min, the emission intensity reached the plateau and hardly increased even with increasing heating time (Figure S31, Supporting Information). At this point, the water in the film is almost removed. At the same time, the lifetime also showed the similar changing tendency: The lifetime was gradually extended with the increase of heating time, reaching a maximum of 2.92 s after heating for 30 min (Figure S32). Subsequently, we explored the cyclic process of spraying water and removing water by heating the P_1/PVA@RhB film for 30 min. The 465 nm emission band's RTP intensity gradually decreased with water spraying. Thus, the property of the film could be controlled by wet/dry stimuli, and multiple cycles can be repeated (Figure 4d).

Owning mechanical flexibility and processability, these supramolecular systems have been successfully applied to information encryption and anti-counterfeiting. The word "NKU" was separately written on the surface of non-fluorescent paper respectively by the solution of P_1/PVA, P_1/PVA@RhB, P_1/PVA@RhB:Cy5 ([P_1]:[RhB]:[Cy5] = 100:20:4, m_{CZ}:m_{PVA} = 50:1). This characters emitted different color under 254 nm UV excitation, and it can be seen with different duration after UV off (**Figure 5**a). In addition, this can be used to construct 2D information encryption based on the characteristics of P_1/PVA, P_1/PVA@RhB, P_1/PVA@RhB:Cy5 films fluorescence and delay time (Figure 5b). Encrypted information of the binary codes of standard 8-bit ASCII characters is written on paper using four types of aqueous solutions, including the solution of P_1/PVA, P_1/PVA@RhB, P_1/PVA@RhB:Cy5 and PVA@RhB. We just can observe "8" by naked eye after writing. In the decryption steps, UV light and delay time are crucial. The fake information was rendered under UV light. After turning off the light, decrypted "DAP" was observed first. Over time, another password, "FCT" emerged. Carefully and patiently observing, it can finally see that "NKU" is the correct password. It is worth mentioning that this code can be destroyed in time after spraying water, but after 10 min of drying, it can be reproduced, and this process can be cycled multiple times.

3. Conclusion

In conclusion, we have constructed a two-step cascaded phosphorescent energy transfer system based on the ternary copolymers. Guest-induced phosphorescence emission and the enrichment of macrocyclic and rigid polymer enable this supramolecular aggregate P_1/PVA system to achieve excellent tandem phosphorescence energy transfer, with a lifetime of 1.07 s at 680 nm and energy transfer efficiency of up to 97.4%. It is anticipated that this supramolecular aggregate will offer a practical and workable strategy for creating cascaded phosphorescent energy transfer systems with long-range and long-lifetime photoluminescence,

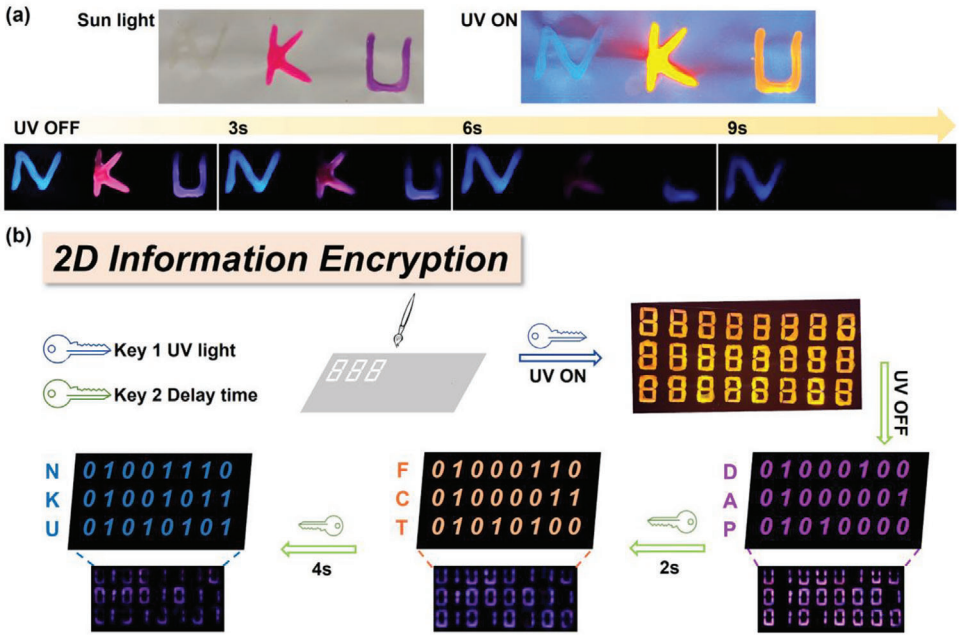

Figure 5. a) Pictures of the "NKU" paper separately written by the solution of P_1/PVA, P_1/PVA@RhB and P_1/PVA@RhB: Cy5 under different light and delayed light; b) A binary code constructed by the solution of P_1/PVA, P_1/PVA@RhB, P_1/PVA@RhB:Cy5 and PVA@RhB papers for 2D information encryption, with UV excitation and delay time as the decryption elements (the molar ratio of P_1/PVA to RhB to Cy5 is 100:20:4, m_{CZ}:m_{PVA} = 50:1).

as well as new opportunities for the development of more sophisticated phosphorescent supramolecular systems for phosphorescence materials studies.

Supporting Information

Supporting Information is available from the Wiley Online Library or from the author.

Acknowledgements

The authors thank the National Natural Science Foundation of China (NNSFC, Grant Nos. 22171148, 22131008) and Natural Science Foundation of Tianjin (21JCZDJC00310) for financial support.

Conflict of Interest

The authors declare no conflict of interest.

Author Contributions

Q.C. and X.-K.M. contributed equally to this work. Y.-M.Z. and Y.L. conceived and designed the experiments. Q.C. and X.-K.M. synthesized and performed the chemical characterization. Q.C. and X.-K.M. wrote the main manuscript. X.Z. gave support to the final version of the manuscript. Y.-M.Z. and Y.L. supervised the work and edited the manuscript. All authors analyzed and discussed the results and reviewed the manuscript.

Data Availability Statement

The data that support the findings of this study are available from the corresponding author upon reasonable request.

Keywords

anti-counterfeiting, cyclodextrin, energy transfer, phosphorescence

Received: October 26, 2023
Revised: November 16, 2023
Published online:

[1] Z. Xie, X. Zhang, H. Wang, C. Huang, H. Sun, M. Dong, L. Ji, Z. An, T. Yu, W. Huang, *Nat. Commun.* **2021**, *12*, 3522.
[2] Z.-Y. Zhang, W.-W. Xu, W.-S. Xu, J. Niu, X.-H. Sun, Y. Liu, *Angew. Chem., Int. Ed.* **2020**, *59*, 18748.
[3] H. Wu, Y. Chen, Y. Liu, *Adv. Mater.* **2017**, *29*, 1605271.
[4] Y.-Y. Hu, X.-Y. Dai, X. Dong, M. Huo, Y. Liu, *Angew. Chem., Int. Ed.* **2022**, *134*, e202213097.
[5] X.-M. Chen, W.-J. Feng, H. K. Bisoyi, S. Zhang, X. Chen, H. Yang, Q. Li, *Nat. Commun.* **2022**, *13*, 3216.
[6] W. Ye, H. Ma, H. Shi, H. Wang, A. Lv, L. Bian, M. Zhang, C. Ma, K. Ling, M. Gu, Y. Mao, X. Yao, C. Gao, K. Shen, W. Jia, J. Zhi, S. Cai, Z. Song, J. Li, Y. Zhang, S. Lu, K. Liu, C. Dong, Q. Wang, Y. Zhou, W. Yao, Y. Zhang, H. Zhang, Z. Zhang, X. Hang, et al., *Nat. Mater.* **2021**, *20*, 1539.
[7] Z.-A. Yan, X. Lin, S. Sun, X. Ma, H. Tian, *Angew. Chem., Int. Ed.* **2021**, *60*, 19735.
[8] C. Wang, Y.-H. Liu, Y. Liu, *Small* **2022**, *18*, 2201821.
[9] A. Ajayaghosh, V. K. Praveen, C. Vijayakumar, S. J. George, *Angew. Chem., Int. Ed.* **2007**, *119*, 6376.
[10] Z. Yu, H. K. Bisoyi, X.-M. Chen, Z.-Z. Nie, M. Wang, H. Yang, Q. Li, *Angew. Chem., Int. Ed.* **2022**, *61*, e202200466.
[11] K. V. Rao, K. K. R. Datta, M. Eswaramoorthy, S. J. George, *Adv. Mater.* **2013**, *25*, 1713.
[12] L. Ma, Q. Xu, S. Sun, B. Ding, Z. Huang, X. Ma, H. Tian, *Angew. Chem., Int. Ed.* **2022**, *61*, e202115748.

[13] H. Wu, Y. Wang, L. O. Jones, W. Liu, B. Song, Y. Cui, K. Cai, L. Zhang, D. Shen, X.-Y. Chen, Y. Jiao, C. L. Stern, X. Li, G. C. Schatz, J. F. Stoddart, *J. Am. Chem. Soc.* **2020**, *142*, 16849.
[14] M. Huo, X.-Y. Dai, Y. Liu, *Angew. Chem., Int. Ed.* **2021**, *60*, 27171.
[15] W.-W. Xing, H.-J. Wang, Z. Liu, Z.-H. Yu, H.-Y. Zhang, Y. Liu, *Adv. Opt. Mater.* **2023**, *11*, 2202588.
[16] F. Lin, H. Wang, Y. Cao, R. Yu, G. Liang, H. Huang, Y. Mu, Z. Yang, Z. Chi, *Adv. Mater.* **2022**, *34*, 2108333.
[17] X. Ma, J. Wang, H. Tian, *Acc. Chem. Res.* **2019**, *52*, 738.
[18] Q. Dang, Y. Jiang, J. Wang, J. Wang, Q. Zhang, M. Zhang, S. Luo, Y. Xie, K. Pu, Q. Li, Z. Li, *Adv. Mater.* **2020**, *32*, 2006752.
[19] X. Zhang, L. Du, W. Zhao, Z. Zhao, Y. Xiong, X. He, P. F. Gao, P. Alam, C. Wang, Z. Li, J. Leng, J. Liu, C. Zhou, J. W. Y. Lam, D. L. Phillips, G. Zhang, B. Z. Tang, *Nat. Commun.* **2019**, *10*, 5161.
[20] X. Zhang, J. Liu, B. Chen, X. He, X. Li, P. Wei, P. F. Gao, G. Zhang, J. W. Y. Lam, B. Z. Tang, *Matter* **2022**, *5*, 3499.
[21] S. Garain, B. C. Garain, M. Eswaramoorthy, S. K. Pati, S. J. George, *Angew. Chem., Int. Ed.* **2021**, *60*, 19720.
[22] M. Huo, X.-Y. Dai, Y. Liu, *Small* **2022**, *18*, e2104514.
[23] F.-F. Shen, Y. Chen, X. Dai, H.-Y. Zhang, B. Zhang, Y. Liu, Y. Liu, *Chem. Sci.* **2020**, *12*, 1851.
[24] W.-W. Xu, Y. Chen, Y.-L. Lu, Y.-X. Qin, H. Zhang, X. Xu, Y. Liu, *Angew. Chem., Int. Ed.* **2022**, *61*, e202115265.
[25] J. Yang, X. Wu, J. Shi, B. Tong, Y. Lei, Z. Cai, Y. Dong, *Adv. Funct. Mater.* **2021**, *31*, 2108072.
[26] S. Kuila, S. J. George, *Angew. Chem., Int. Ed.* **2020**, *59*, 9393.
[27] W. Zhao, T. S. Cheung, N. Jiang, W. Huang, J. W. Y. Lam, X. Zhang, Z. He, B. Z. Tang, *Nat. Commun.* **2019**, *10*, 1595.
[28] Z. Liu, Y. Liu, *Chem. Soc. Rev.* **2022**, *51*, 4786.
[29] Y. Gong, G. Chen, Q. Peng, W. Z. Yuan, Y. Xie, S. Li, Y. Zhang, B. Z. Tang, *Adv. Mater.* **2015**, *27*, 6195.
[30] K. Ogawa, F. Guo, K. S. Schanze, *J. Photochem. Photobiol. A* **2009**, *207*, 79.
[31] S. Liu, X. Fang, B. Lu, D. Yan, *Nat. Commun.* **2020**, *11*, 4649.
[32] W. Lin, Q. Tan, H. Liang, K. Y. Zhang, S. Liu, R. Jiang, R. Hu, W. Xu, Q. Zhao, W. Huang, *J. Mater. Chem. C* **2015**, *3*, 1883.
[33] P. M. Gewehr, D. T. Delpy, *Med. Biol. Eng. Comput.* **1993**, *31*, 2.
[34] Y. Zeng, Y. Li, M. Li, G. Yang, Y. Li, *J. Am. Chem. Soc.* **2009**, *131*, 9100.
[35] S. T. J. Ryan, J. Del Barrio, I. Ghosh, F. Biedermann, A. I. Lazar, Y. Lan, R. J. Coulston, W. M. Nau, O. A. Scherman, *J. Am. Chem. Soc.* **2014**, *136*, 9053.
[36] S. T. J. Ryan, R. M. Young, J. J. Henkelis, N. Hafezi, N. A. Vermeulen, A. Hennig, E. J. Dale, Y. Wu, M. D. Krzyaniak, A. Fox, W. M. Nau, M. R. Wasielewski, J. F. Stoddart, O. A. Scherman, *J. Am. Chem. Soc.* **2015**, *137*, 15299.
[37] X.-K. Ma, Y. Liu, *Acc. Chem. Res.* **2021**, *54*, 3403.
[38] M. Constantin, S. Bucatariu, P. Ascenzi, B. C. Simionescu, G. Fundueanu, *React. Funct. Polym.* **2014**, *84*, 1.
[39] Z. Deng, Y. Guo, X. Zhao, P. X. Ma, B. Guo, *Chem. Mater.* **2018**, *30*, 1729.
[40] H.-Q. Peng, L.-Y. Niu, Y.-Z. Chen, L.-Z. Wu, C.-H. Tung, Q.-Z. Yang, *Chem. Rev.* **2015**, *115*, 7502.
[41] Z. Xu, S. Peng, Y.-Y. Wang, J.-K. Zhang, A. I. Lazar, D.-S. Guo, *Adv. Mater.* **2016**, *28*, 7666.
[42] X. Zhu, J.-X. Wang, L.-Y. Niu, Q.-Z. Yang, *Chem. Mater.* **2019**, *31*, 3573.
[43] D. Li, J. Yang, M. Fang, B. Z. Tang, Z. Li, *Sci. Adv.* **2022**, *8*, eabl8392.
[44] X. Zhang, Y. Cheng, J. You, J. Zhang, Y. Wang, J. Zhang, *ACS Appl. Mater. Interfaces* **2022**, *14*, 16582.
[45] X. Wang, Y. Xu, X. Ma, H. Tian, *Ind. Eng. Chem. Res.* **2018**, *57*, 2866.
[46] J. Yang, M. Fang, Z. Li, *Acc. Mater. Res.* **2021**, *2*, 644.
[47] J.-J. Li, H.-Y. Zhang, Y. Zhang, W.-L. Zhou, Y. Liu, *Adv. Opt. Mater.* **2019**, *7*, 1900589.
[48] D. Li, Y. Yang, J. Yang, M. Fang, B. Z. Tang, Z. Li, *Nat. Commun.* **2022**, *13*, 347.